Performance Enhancement of Wind Farms Using Tuned SSSC Based on Artificial Neural Network

Yousry Ibrahim[1], Salah Kamel[1,2], Ahmed Rashad[1], Loai Nasrat[1], Francisco Jurado[3]*

[1] Department of Electrical Engineering, Faculty of Engineering, Aswan University, 81542 Aswan (Egypt)
[2] Department of Electrical Engineering, University of Jaén, 23700 EPS Linares, Jaén (Spain)
[3] State Key Laboratory of Power Transmission Equipment and System Security and New Technology, Chongqing University, Chongqing 400030 (China)

Received 4 December 2018 | Accepted 1 May 2019 | Published 9 May 2019

Abstract

Recently, power systems are confronting a lot of challenges. Increasing the dependence on renewable energy sources especially wind energy and its impact on the stability of electrical systems are the most important challenges. Flexible alternating current transmission systems (FACTS) can be used to improve the relationship between wind farms and electrical grids. The performance of these FACTS depends on the parameters of its control system. These parameters can be tuned using modern methods like Artificial Neural Network (ANN). In this paper, ANN is used to improve the performance of static synchronous series compensator (SSSC) integrated into combined wind farm (CWF). This CWF is composed of squirrel cage induction generators (SCIG) and doubly fed induction generators (DFIG) wind turbines. This wind farm is collecting the advantage of SCIG and DFIG wind turbines. To view out the motivation of this paper, a comparison is done among the performances of combined wind farm (CWF) with ANN-SSSC, CWF with ordinary SSSC and CWF with SSSC tune by Multi-objective genetic algorithm (MOGA SSSC). The root mean square Error (RMSE) is used to evaluate the results. The results illustrate that the performance of CWF can be improved using SSSC adjusted by ANN.

Keywords

Squirrel Cage Induction Generator (SCIG), Doubly Fed Induction Generator (DFIG), Combined Wind Farm (CWF), Static Synchronous Series Compensator (SSSC), Artificial Neural Network (ANN).

DOI: 10.9781/ijimai.2019.05.001

I. Introduction

Renewable energy is an important source for the power generation. Solar energy, and wind energy are the most famous forms of this technology. Wind energy plays an important role in producing electric power in all the world so that its injection on the grid represents a wide range of studies. This injection depends on the induction generator of the wind turbines. There are two types of induction generator, first type is squirrel cage induction generators (SCIG) which are suitable to fixed speed wind turbines and second type is doubly fed induction generators (DFIG) that are used with variable speed wind turbines. The stability of wind farms is affected by the exchange in the reactive power between the interconnected grid and the wind farms. The compensation devices of the reactive power consider a fundamental element in SCIG wind turbines (SCIG-WT). The flexible alternating current transmission systems (FACTS) were used to damp power oscillation and, enhance power stability. In Ref. [1] a dual STATCOM had been used to damp power oscillations. Tuning parameters of SSSC had been proposed in [2] to damp power oscillations. In Ref [3] a unified power flow controller has been used to damp power oscillations between two areas. The SSSC used to damp power oscillation, enhance power stability and control the power flow of DFIG-WF is studied in [4]-[5].The effect of FACTS such as Static VAR Compensator (SVC), Static Synchronous Compensator (STATCM) and SSSC on the performance of wind farms were studied in [6]-[10]. The impact of SSSC on the performance of different types of wind farms had been discussed in [11].

The main advantage of Artificial intelligence (AI) is solving complex problems in less time and with high precision, such as using optimization methods to solve the complex control problem. Also, AI can easily predict and take the correct decisions with little margin of error. It can be used for predicting the change in wind speed and its impact on stability of power system. In this paper, AI has been used to predict and determine the optimal value of the control gains of SSSC which can enhance the performance of CWF. On other side, AI represents high technology so that it is storage costly. In last years, Artificial Intelligence (AI) has been used extensively in improving the performance of FACTS and enhancing the performance of wind farms interconnected grid. A genetic algorithm has been implemented to tune different type of FACTS interconnected wind farms and photovoltaic solar plant in [12]. In ref [13] [14] multi-objective genetic algorithm is used to improve the performance of DFIG. Also, multi-objective genetic algorithm is used to find the optimal gains of SSSC in [15]. Adaptive-network-based fuzzy inference system (ANFIS), ANN and genetic algorithm are proposed in [16] to improve the reactive power control of STATCOM. The whale optimization algorithm, genetic algorithm and ANN were used in [17] to determine the optimal parameters of STATCOM integrated with CWF. In Ref [18] particle swarm optimization is used to tune and damp power system oscillation of DFIG wind farms integrated with SSSC. A new control strategy based on ANFIS is proposed in [19] to improve the performance of DFIG wind farm integrated with SSSC.

* Corresponding author.
E-mail address: fjurado@ujaen.es

This paper aims to improve the performance of CWF which is based on SCIG and DFIG using SSSC controlled by ANN (ANN-SSSC). Also, in this paper the control parameters which had been investigated in [15] are used for implementing ANN. Moreover, a comparison is done between the performances of CWF with ordinary SSSC, CWF associated with SSSC tuned by multi-objective genetic algorithm (SSSC MOGA) investigated in [15] and CWF associated with proposed ANN-SSSC during three phase-faults.

The rest of the paper is organized as follows. Section II presents a brief summary of ANN. Section III presents modelling of wind turbines. Section IV explains the construction, operation and control system of SSSC. Section V introduces the proposed ANN control, which is applied to SSSC. The last two sections present the results and conclusion.

II. Artificial Neural Network (ANN)

The artificial neural network is a modest simulation of the effect, form and content of the neural network found in the human brain. It consists of nodes called neurons and connected together by bonds called weights. Each set of neurons forms a single layer; the ANN is composed of different types of layers. From Fig. 1, it can be observed that it consists of input layer, hidden layer (processing element) and output layer. The hidden layer could be single layer or multi-layers. The input signal is passed from input layer to the output layer through the hidden layer. The input is transferred to the neurons through weight matrix W. The output can be given by [20]:

$$Y_{out} = \sum_{j=1\to n}^{i=1\to n} x_i w_{ji} \quad (1)$$

Where Y_{out} represents the output of ANN, x is input signal which starts from 1 to n inputs and w_{ji} represents the synaptic weights between neurons.

III. Modeling of Wind Turbines

The mathematical model of wind turbines was discussed in several articles on wind energy. Fig. 2 shows the equivalent circuit of induction generator. The direct and quadratic (d-q) illustration of IG with respect to the synchronous frame can be illustrated as flows [21] [22]:

$$\begin{cases} v_{ds} = p\varphi_{ds} - \omega_s\varphi_{qs} + R_s i_{ds} \\ v_{qs} = p\varphi_{qs} - \omega_s\varphi_{ds} + R_s i_{qs} \end{cases} \quad (2)$$

$$\begin{cases} v_{dr} = p\varphi_{dr} - s\omega_s\varphi_{qr} + R_r i_{dr} \\ v_{qr} = p\varphi_{qr} - s\omega_s\varphi_{dr} + R_r i_{qr} \end{cases} \quad (3)$$

$$\begin{bmatrix} \varphi_{ds} \\ \varphi_{qs} \\ \varphi_{dr} \\ \varphi_{qr} \end{bmatrix} = \begin{bmatrix} i_{ds} \\ i_{qs} \\ i_{dr} \\ i_{qr} \end{bmatrix} \cdot \begin{bmatrix} (L_{ls}+L_m) & 0 & L_m & 0 \\ 0 & (L_{ls}+L_m) & 0 & L_m \\ L_m & 0 & (L_{lr}+L_m) & 0 \\ 0 & L_m & 0 & (L_{lr}+L_m) \end{bmatrix} \quad (4)$$

$$\begin{bmatrix} i_{ds} \\ i_{qs} \\ i_{dr} \\ i_{qr} \end{bmatrix} = \frac{1}{(L_{ls}+L_m)(L_{lr}+L_m)-L_m^2} \begin{bmatrix} (L_{lr}+L_m) & 0 & -L_m & 0 \\ 0 & (L_{lr}+L_m) & 0 & -L_m \\ -L_m & 0 & (L_{ls}+L_m) & 0 \\ 0 & -L_m & 0 & (L_{ls}+L_m) \end{bmatrix} \cdot \begin{bmatrix} \varphi_{ds} \\ \varphi_{qs} \\ \varphi_{dr} \\ \varphi_{qr} \end{bmatrix} \quad (5)$$

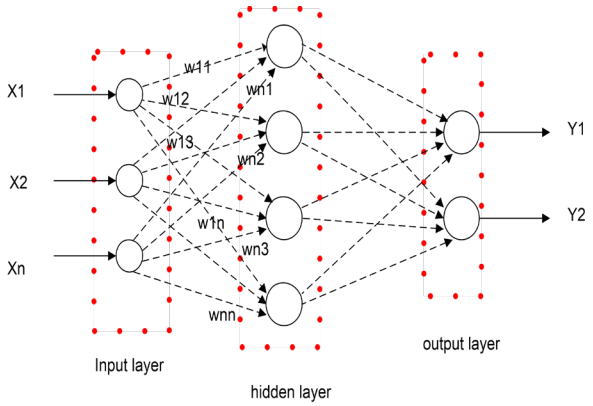

Fig. 1. ANN principle operation.

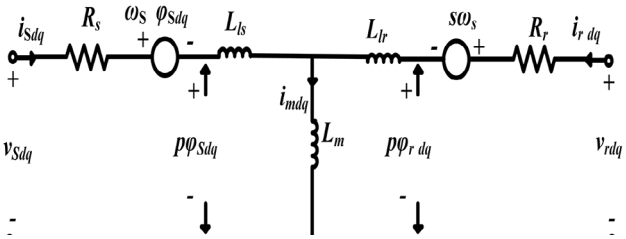

Fig. 2. Equivalent circuit of IG generators.

Equations (2) to (5) and Fig. 2 can be applied to a general modeling of IG. The voltage of rotor of SCIG is equal to zero because the rotor is a short circuit and there is no connection between SCIG's rotor and the grid as shown in Fig. 3 (a). While the rotor in DFIG is a wound rotor so the rotor current and voltage is taken into account. The AC/DC/AC converters are used to connect rotor of DFIG's to the grid through as illustrated in Fig. 3 (b). The equivalent circuits of DFIG and SCIG are illustrated in Fig. 3 (c) and (d).

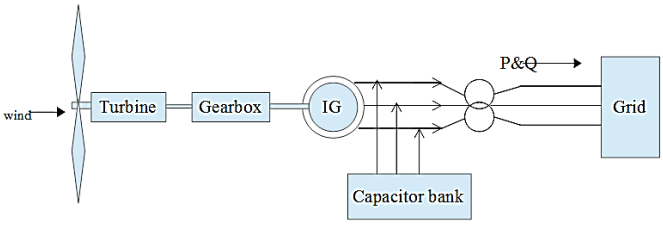

(a) A block diagram of SCIG interconnected grid

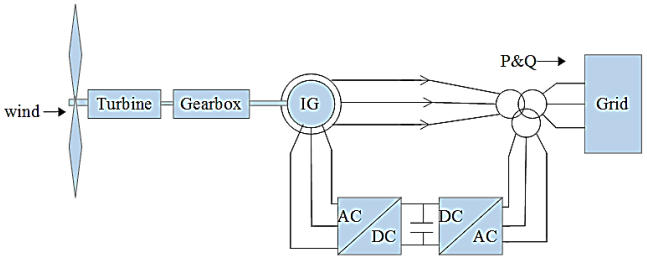

(b) A block diagram of DFIG interconnected grid

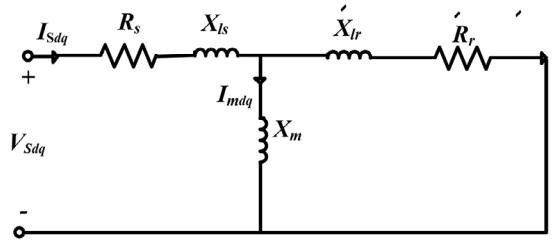

(c) Equivalent circuit of SCIG during steady stat

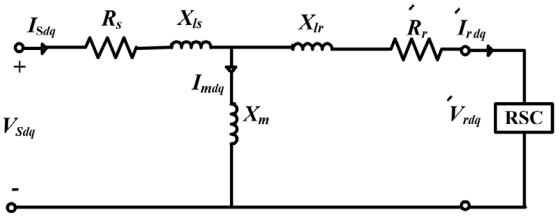

(d) Equivalent circuit of DFIG during steady stat

Fig. 3. Equivalent circuits and block diagrams of SCIG and DFIG.

The extracted power from the wind by wind farms is given by:

$$P_{wt} = \frac{1}{2}\rho A v^3 C_p$$

$$C_p = 0.517\left(\frac{116}{\lambda_i} - 0.4\beta - 5\right)e^{\frac{-0.0068}{\lambda_i}} + 0.0068\lambda$$

$$\frac{1}{\lambda_i} = \frac{1}{116}\left(\frac{1}{\lambda+0.08\beta} - \frac{0.035}{\beta^3+1}\right)$$

$$\lambda = \frac{\omega_r l_b}{v} \tag{6}$$

Where, v is the wind speed, ρ is the air density, C_p is the power coefficient, A is the area swept by the turbine blades. l_b is the blade length or rotor radius, ω_r is the rotor speed and it is equal to1.22Kg/m3. C_p is a function on the pitch angle β and the tip speed ratio λ.

The electrical torque of SCIG and DFIG is given by:

$$T_e = \frac{3PL_m}{2L_r}\left(i_{qs}\varphi_{dr} - i_{ds}\varphi_{qr}\right) \tag{7}$$

$$T_e = \frac{3P}{2}\left(i_{qs}\varphi_{ds} - i_{ds}\varphi_{qs}\right) \tag{8}$$

The pitch angle control method is used to control the rotor speed of wind turbine in order to keep the output power inside permissible limits. Fig. 4 illustrates a schematic diagram of pitch angle control system [23].

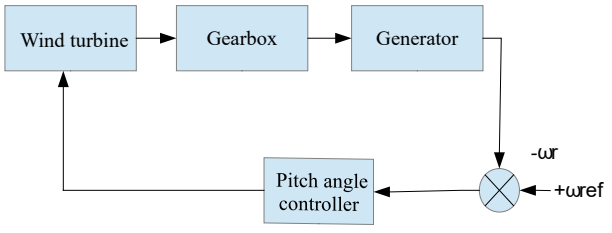

Fig. 4. A block diagram of pitch angle control system.

IV. Static Synchronous Series Compensator (SSSC)

The Static Synchronous Series Compensator (SSSC) belongs to the series devices of FACTS controller [23]. It is a series connected with the transmission line so that it injects a series voltage which is in phase quadrature with the line current. The block diagram of SSSC and its equivalent circuit are shown in Fig. 5. As shown in Fig. 5. The SSSC is connected in series with the transmission line of an electrical grid by a coupling transformer.

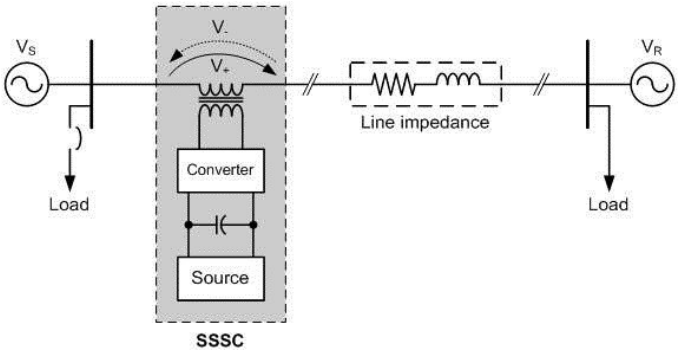

(a) Schematic diagram of SSSC

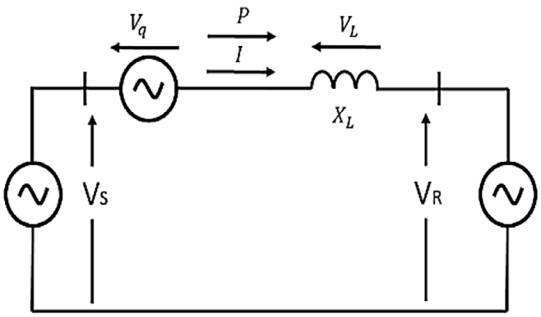

(b) Equivalent circuit of SSSC

Fig. 5. Principle operation of SSSC.

As shown in Fig. 5 (b) the SSSC injects voltage in series with the line. This voltage injected may be capacitive or inductive, if the injection voltage overrides the voltage drop (VL), the transferred power will be reflected in the direction.

A. SSSC Control System

The main components of SSSC controller are AC voltage regulator and DC voltage regulator. Fig. 6 (a) shows the MATLAB Simulink model of ordinary SSSC control system. Fig. 6 (b) illustrates the PI controller of AC voltage regulator and DC voltage of ordinary SSSC. The initial values of AC voltage (Kp_Vac and Ki_Vac) and gains of DC voltage (Kp_Vdc, Ki_Vdc) are specified by MATLAB Simulink model.

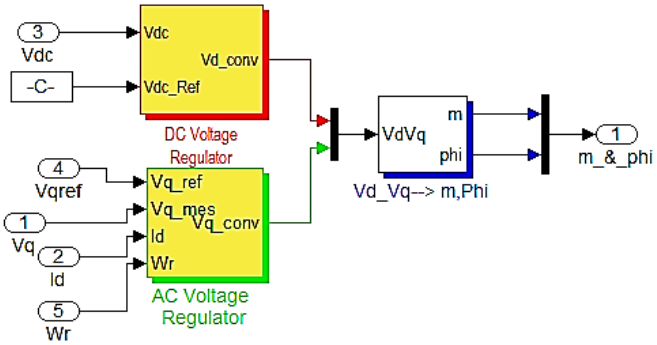

(a) MATLAB model of SSSC control system

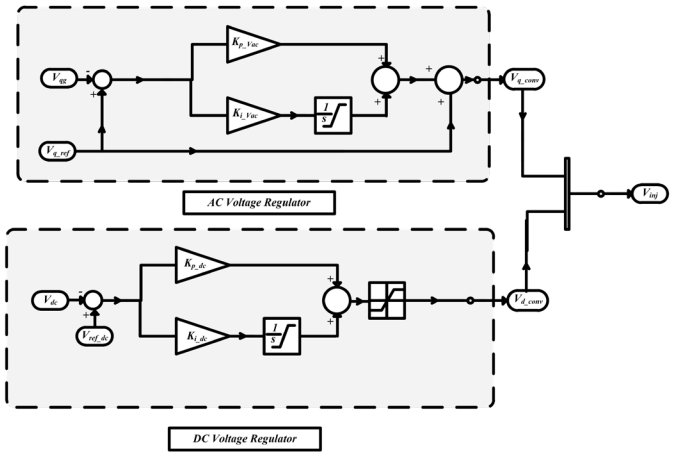

(b) PI controller of DC and AC voltage regulators

Fig. 6. SSSC controller.

V. Applying the ANN Method

In this work the ANN is based on multi-layer feed-forward network. The multi-layer is divided into three layers input, hidden and output layer. Fig. 7 represents the flowchart of adjusting SSSC's parameters using ANN. As shown in Fig. 7, the neural fitting tool (NFTOOL) and the sample range are based on the value of control parameters of SSSC tuned by multi-objective genetic algorithm (SSSC MOGA) investigated in [15]. Also, Fig. 7 illustrates that the input signal is the change in voltage at the point of connection and the output layer represents the control parameters of SSSC (AC voltage regulator (Kp-vac and Ki-vac) and DC voltage regulator (Kp-vdc and Ki-vdc)). In this work, Levenberg-Marquardt algorithm is used for training the value of control parameters of SSSC tuned by multi-objective genetic algorithm (SSSC MOGA) investigated in [15].

The neural fitting tool (NFTOOL) is composed of sets of processes: training, validation and testing. The application divides input and target into three groups as follows: 70% is applied for training. 15% is applied to validate and 15% is applied to test. Table I shows the parameters of NFTOOL and illustrates the mean square error (MSE) and regression value (R) of training, validation and testing.

TABLE I. The Value of Gains of AC Voltage, DC Voltage Regulators Obtained Using Moga

Process	Selected percentage	Number of samples	MES	R value
training,	70%	6385	4.790e-5	1.859e-1
validation	30%	1362	4.8334e-5	1.909e-1
testing	30%	1362	4.8614e-5	1.826e-1
Type of algorithm	Levenberg-Marquardt and multi-objective genetic algorithm investigated in [15]			
Number of hidden neurons	20 neurons			

In this study NFTOOL is a feed forward network with input, output and multi-layers. Fig. 8 (a) illustrates the neural network size. Fig. 8 (b) illustrates training, validation and testing samples. Fig. 8 (c) illustrates results of training operation. Fig. 9 illustrates best validation performance. Fig. 10 illustrates the ANN controller of DC and AC voltage regulators.

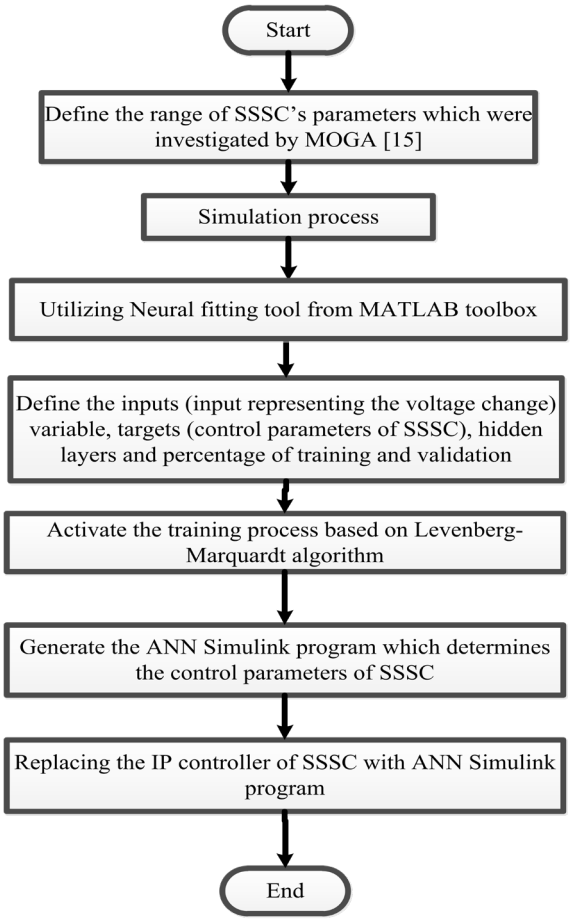

Fig. 7. The flow chart of adjusting SSSC's parameters using ANN operation.

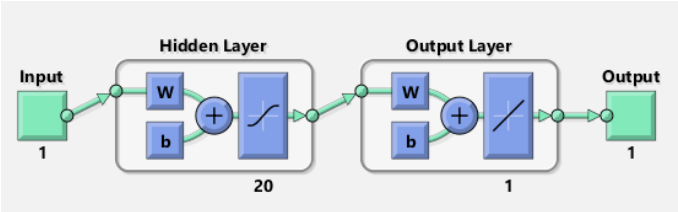

(a) Neural network size

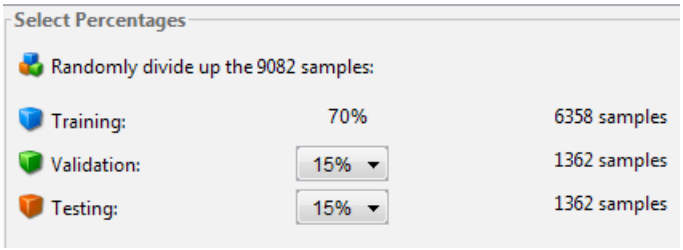

(b) Training, Validation and testing samples

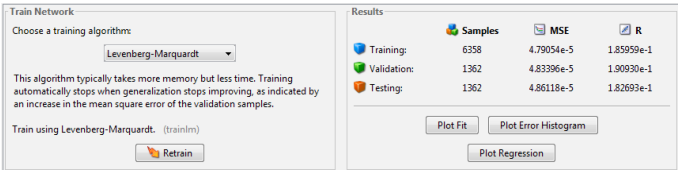

(c) Results of training operation

Fig. 8. The size, training operation and the results.

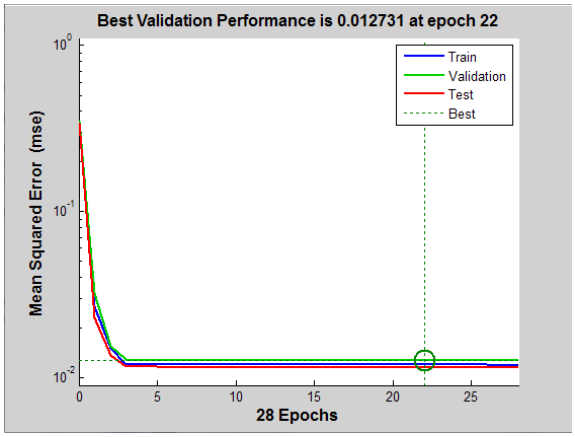

Fig. 9. The performance's convergence of the studied system with ANN.

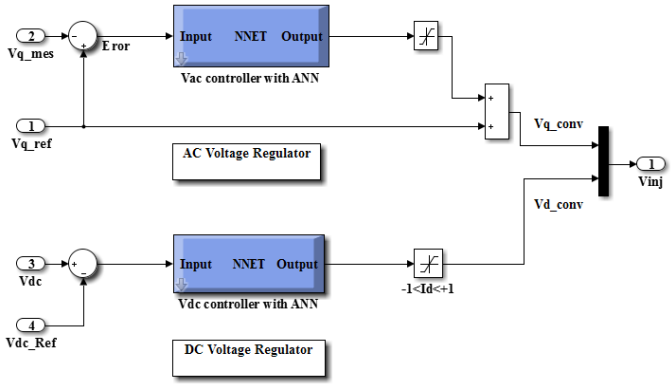

Fig. 10. ANN controller of DC and AC voltage regulators.

VI. Studied System Description

The studied system contains six wind turbines, each one produces 1.5 MW and 575v. The wind turbines are divided into three SCIG fixed-speed wind turbines and three DFIG variable speed wind turbines. Fig. 11 shows the block diagram of the studied system. A three phase fault is applied at 25 s and removes [e1] the fault after time equal 25.15 s.

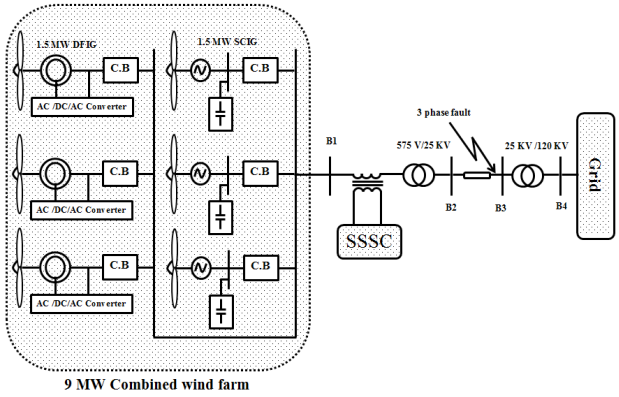

Fig.11. The block diagram of the system.

VII. Simulation Results

The simulation studied the performance of CWF with ANN-SSSC and CWF with ordinary SSSC (PI-SSSC) during three-phase fault. The voltage, reactive power and active power are measured at the point connection between the interconnected grid and wind farms.

The value of the control parameters of ordinary SSSC, MOGA SSSC and the proposed ANN SSC are shown in Table II.

TABLE II. The Value Of Gains of AC Voltage, DC Voltage Regulators of Ordinary SSSC, SSSC Moga and Ann SSSC

Type of SSSC	Regulator	Gain	Gain value
ordinary SSSC	AC voltage	Kp_Vac, Ki_Vac,	3.75e-3 0.1875
	DC voltage	Kp_Vdc, Ki_Vdc,	0.1e-3 20e-3
MOGA SSSC	AC voltage	Kp_Vac, Ki_Vac,	0.24742 0.98783
	DC voltage	Kp_Vdc Kp_Vdc,	0.06939. 0.95957
proposed ANN SSC	AC voltage	Kp_Vac, Ki_Vac,	0.1107 0.8665
	DC voltage	Kp_Vdc Kp_Vdc,	0.0753 0.8686

A. Impact of Three Fault

As illustrated in Fig. 12 the voltage with ANN-SSSC is 0.81 pu while the voltage with ordinary SSSC is 0.73 pu and the voltage with MOGA-SSSC is 0.75 pu. This means that the voltage of CWF has been improved with ANN-SSSC more than with the ordinary SSSC.

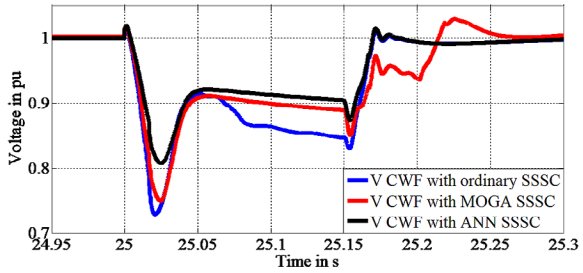

Fig. 12. The voltage of CWF with ANN-SSSC and CWF with ordinary SSSC during three phase fault.

This enhancement in voltage of CWF with ANN SSSC is due to the enhancement in the performance of SSSC when it is controlled by ANN. This can be observed by monitoring the injected voltage of SSSC in case of ordinary, MOGA and ANN as shown in Fig. 13.

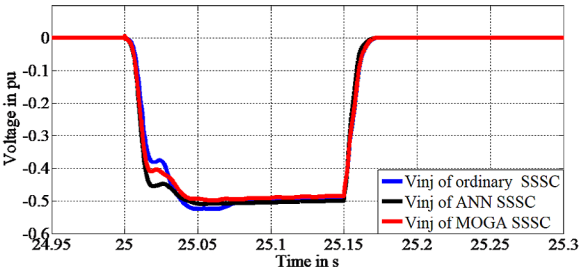

Fig. 13. The injected voltage of SSSC in case of ordinary, MOGA and ANN.

As illustrated in Fig. 14, the injected voltage of SSSC has been increased when it is controlled by ANN specially at the begging of fault period. This will decrease the reactive power absorbed by the CWF with ANN SSSC during fault.

As illustrated in Fig. 14 the reactive power of CWF with ANN-SSSC is-2.8 MVAR while the reactive power with ordinary SSSC is -4.75 MVAR and -3.83 MVAR for MOGA SSSC especially at the beginning of fault period. This means that the performance of CWF has been improved with ANN-SSSC more than the ordinary SSSC.

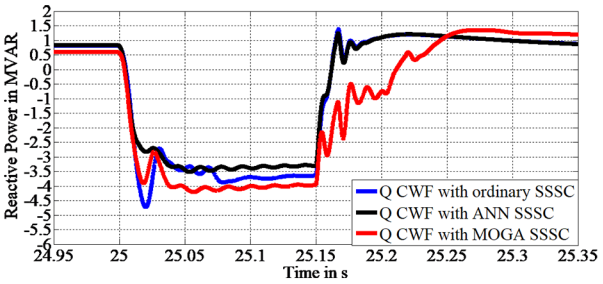

Fig. 14. The reactive power of CWF with ANN-SSSC and CWF with ordinary SSSC during three phase fault.

As illustrated in Fig. 15 the active power of CWF with ANN-SSSC has the highest value of output power especially at the beginning of fault period.

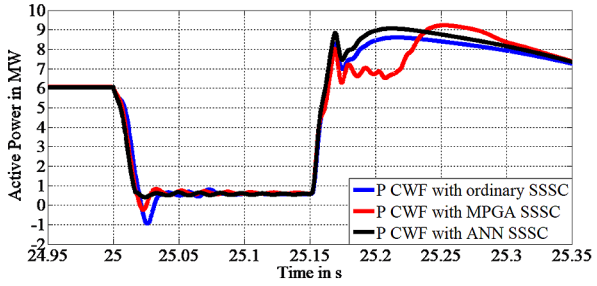

Fig. 15. The active power of CWF with ANN-SSSC and CWF with ordinary SSSC during three phase fault.

In order to justify the good performance of the proposed method, root mean square Error (RMSE) is used to measure the impact of ordinary SSSC, MOGA SSSC and ANN SSSC on the performance of CWF during the fault. RMSE is used to measure the error between the reference voltage (Vref = 1 pu) and the actual voltage at the point of common connection during the fault condition. Table III shows the RMSE of the three cases during fault period and after fault clearance.

TABLE III. The Value of RMSE During Fault Period and After Fault Clearance

Period	Ordinary SSSC	MOGA SSSC	ANN SSSC
RMSE during fault period	0.2063	0.1959	0.1805
RMSE after fault clearance	0.1918	0.1721	0.1405

From Table III, it can be observed that the CWF with ANN SSSC has the lowest RMSE. This means that the ANN managed to tune SSSC and gives the best result.

VIII. Conclusions

This paper has presented the design of a CWF which consists of two types of induction generator, the first one is SCIG fixed speed wind turbines and the second one is DFIG variable speed wind turbines. ANN has been used in order to adjust SSSC's parameters to enhance the performance of combined wind farm (CWF). In addition, this paper includes a comparison among the performances of combined wind farm (CWF) with ANN-SSSC, with performances of CWF with ordinary SSSC and performances of CWF with SSSC tune by Multi-objective genetic algorithm (MOGA SSSC). The performances of CWF with ANN-SSSC, ordinary and SSSC MOGA SSSC have been studied during the three-phase fault. The obtained results showed that the adjusted SSSC using ANN had enhanced the active power, the voltage and the reactive power of CWF, particularly during the three-phase fault.

IX. Future Work

This paper opens the door for many future works, for example:

1. Using ANN hybrid with different methods of optimization to determine optimal values for different types of FACTS to improve the performance of wind stations.
2. Use different types of ANN like ANFIS with different methods of optimization to determine optimal values for different types of FACTS to improve wind station performance.

Acknowledgment

The authors gratefully acknowledge the contribution of the NSFC (China)-ASRT (Egypt) Joint Research Fund, Project No. 51861145406 for providing partial research funding to the work reported in this research.

References

[1] D. Ananth and G. N. Kumar, "Mitigation of voltage dip and power system oscillations damping using dual STATCOM for grid connected DFIG," *Ain Shams Engineering Journal,* 2015.

[2] M. G. Jolfaei, A. M. Sharaf, S. M. Shariatmadar, and M. B. Poudeh, "A hybrid PSS–SSSC GA-stabilization scheme for damping power system small signal oscillations," *International Journal of Electrical Power & Energy Systems,* vol. 75, pp. 337-344, 2016.

[3] D. Ananth, G. N. Kumar, D. D. Chowdary, and K. A. Naidu, "Damping of Power System Oscillations and Control of Voltage Dip by Using STATCOM and UPFC." International Journal of Pure and Applied Mathematics, vol.114(10), pp 487-496, August 2017.

[4] P. Bhatt, "Short term active power support from DFIG with coordinated control of SSSC and SMES in restructured power system," in *Power and Energy Engineering Conference (APPEEC), 2014 IEEE PES Asia-Pacific*, 2014, pp. 1-6.

[5] L. Wang and Q.-S. Vo, "Power flow control and stability improvement of connecting an offshore wind farm to a one-machine infinite-bus system using a static synchronous series compensator," *IEEE transactions on sustainable energy,* vol. 4, pp. 358-369, 2013.

[6] H. Heydari-Doostabad, M. R. Khalghani, and M. H. Khooban, "A novel control system design to improve LVRT capability of fixed speed wind turbines using STATCOM in presence of voltage fault," *International Journal of Electrical Power & Energy Systems,* vol. 77, pp. 280-286, 2016.

[7] B. Boubekeur, A. Gherbi, and H. Mellah, "Application of STATCOM to increase transient stability of wind farm," *American Journal of Electrical Power and Energy Systems,* vol. 2, pp. 50-56, 2013.

[8] R. M. Pereira, C. M. Ferreira, and F. M. Barbosa, "Comparative study of STATCOM and SVC performance on dynamic voltage collapse of an electric power system with wind generation," *IEEE Latin America Transactions,* vol. 12, pp. 138-145, 2014.

[9] H. A. Mohammadpour, A. Ghaderi, H. Mohammadpour, and M. H. Ali, "Low voltage ride-through enhancement of fixed-speed wind farms using series FACTS controllers," *Sustainable Energy Technologies and Assessments,* vol. 9, pp. 12-21, 2015.

[10] A. M. Rashad and S. Kamel, "Enhancement of Hybrid Wind Farm performance using tuned SSSC based on Multi-Objective Genetic Algorithm," in *Power Systems Conference (MEPCON), 2016 Eighteenth International Middle East*, 2016, pp. 786-791.

[11] A. Rashad, S. Kamel, and F. Jurado, "Stability improvement of power systems connected with developed wind farms using SSSC controller," *Ain Shams Engineering Journal,* 2017.

[12] O. Nadjemi, T. Nacer, A. Hamidat, H. Salhi, " Optimal hybrid PV/wind energy system sizing: Application of cuckoo search algorithm for Algerian dairy farms," Renewable and Sustainable Energy Reviews, vol 70, April

2017, pp 1352-1365.

[13] Elkasem A. H. A., S. Kamel, A. Rashad, and F. Jurado, "Optimal Performance of Doubly Fed Induction Generator Wind Farm Using Multi-Objective Genetic Algorithm," *International Journal of Interactive Multimedia and Artificial Intelligence,* vol. In Press, pp. 1-6, April 2019.

[14] A. H. Elkasem, S. Kamel, A. Rashad, and F. Jurado, "Optimal Performance of DFIG Integrated with Different Power System Areas Using Multi-Objective Genetic Algorithm," in *2018 Twentieth International Middle East Power Systems Conference (MEPCON)*, 2018, pp. 672-678.

[15] A. M. Rashad and S. Kamel, "Enhancement of Hybrid Wind Farm performance using tuned SSSC based on Multi-Objective Genetic Algorithm," in *2016 Eighteenth International Middle East Power Systems Conference (MEPCON)*, 2016, pp. 786-791.

[16] N. K. Saxena and A. Kumar, "Reactive power control in decentralized hybrid power system with STATCOM using GA, ANN and ANFIS methods," *International Journal of Electrical Power & Energy Systems,* vol. 83, pp. 175-187, 2016.

[17] A. Rashad, S. Kamel, F. Jurado, M. Abdel-Nasser, and K. Mahmoud, "ANN-Based STATCOM Tuning for Performance Enhancement of Combined Wind Farms," *Electric Power Components and Systems,* pp. 1-17, 2019.

[18] J. Bhukya and V. Mahajan, "Optimization of damping controller for PSS and SSSC to improve stability of interconnected system with DFIG based wind farm," *International Journal of Electrical Power & Energy Systems,* vol. 108, pp. 314-335, 2019.

[19] D.-N. Truong and V.-T. Ngo, "Designed damping controller for SSSC to improve stability of a hybrid offshore wind farms considering time delay," *International Journal of Electrical Power & Energy Systems,* vol. 65, pp. 425-431, 2015.

[20] B. Minasny and A. McBratney, "The neuro-m method for fitting neural network parametric pedotransfer functions," *Soil Science Society of America Journal,* vol. 66, pp. 352-361, 2002.

[21] B. Wu, Y. Lang, N. Zargari, and S. Kouro, *Power conversion and control of wind energy systems*: John Wiley & Sons, 2011.

[22] M. G. Simoes and F. A. Farret, *Alternative energy systems: design and analysis with induction generators* vol. 13: CRC press, 2011.

[23] Z. Chen, "Wind turbine drive train systems," *Wind Energy Systems, Optimising design and construction for safe and reliable operation,* pp. 208-246, 2010.

Yousry Ibrahim

Yousry Ibrahim received the B.Eng. from Faculty of Engineering, Aswan University, Egypt in 2013. He is currently pursuing his MSc degree in Department of Electrical Engineering, Aswan Faculty of Engineering, Aswan University. His research activities include renewable energy and power system optimization.

Salah Kamel

Salah Kamel received the international PhD degree from University of Jaen, Spain (Main) and Aalborg University, Denmark (Host) in Jan. 2014. He is an Assistant Professor in Electrical Engineering Department, Aswan University. Also, he is a leader for power systems research group in the Advanced Power Systems Research Laboratory (APSR Lab), Aswan, Egypt. He is currently a Postdoctoral Research Fellow in State Key Laboratory of Power Transmission Equipment and System Security and New Technology, School of Electrical Engineering, Chongqing University, Chongqing, China. His research activities include power system modeling, analysis and simulation, and applications of power electronics to power systems and power quality.

Ahmed Rashad

Ahmed Rashad received the B.Eng. from Faculty of Energy Engineering, Aswan University, Egypt and M.Sc. degree in electrical power engineering from Faculty of Engineering, South Valley University, Egypt in 2013. He is currently pursuing his jointly-supervised Ph.D. degree in Department of Electrical Engineering, Aswan Faculty of Engineering, Aswan University, Egypt and University of Jaen, Linares, Jaen, Spain. His research activities include power system modeling, analysis and simulation, renewable energy and smart grid technologies, applications of power electronics to power systems and power quality.

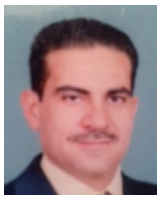

Loai Saad Eldeen Nasrat

Loai Saad Eldeen Nasrat received his B.Sc, M.Sc, and Ph.D degrees in Electrical Engineering from Ain Shams University, Egypt in 1988, 1994, and 1999, respectively. He received a Diploma in Computers and Programming from American University in Cairo, 1994. Since 2002, he has been associated with the Department of Electrical Engineering, Aswan University, Egypt as an Assistant Professor, and since 2008, as an Associate Professor, and since 2013, as a Professor. He is the Vice Dean of Faculty of Engineering for Students and Education Affaires, Aswan University, 2008- till present and the Head of electrical engineering department, Faculty of Engineering, Aswan University from 2006 to 2008. He is currently the Dean of Faculty of Engineering, Aswan University, Egypt. He worked as a part time professor in various Egyptian universities; October 6 University, Alfauom University, Arab Academy for Science, Technology & Maritime Transport, Cinema High Institute, Alazhar University, New Cairo Academy. His research interests include power systems quality and renewable energy.

Francisco Jurado

Francisco Jurado obtained the MSc and PhD degrees from the UNED, Madrid, Spain, in 1995 and 1999 respectively. He is Full Professor at the Department of Electrical Engineering of the University of Jaén, Spain. His research activities have focused on two topics: power systems and renewable energy.